Supplementary Material for

Dynamic Path Exploration on Mobile Devices

1 Occlusion Function

To evaluate $o(L_i(x_c,y_c))$, we leverage the vector data we downloaded from the OSM database and render all containing roads into a grayscale image buffer B whose extent is chosen according to the map area of the cell domain and whose resolution is chosen to resemble the resolution of the output device. Since roads are encoded in the OSM as simple polylines, for simplicity reasons we choose a constant line thickness for all roads that corresponds to a road width of 8 meters. We use two different gray values: Road segments which correspond to the path $\mathbf{p}(t)$ are drawn in pure white (1.0). For all other roads we choose a darker color to indicate their smaller importance (usually 0.25). Areas which do not belong to roads remain black (0.0).

In order to compute $o(L_i(x_c,y_c))$ for a detail lens L_i that is placed at a cell c inside the domain, we evaluate the corresponding pixel extent of the detail lens in the grayscale image buffer B and denote the pixel coordinates in B defining this extent as $\mathrm{x}^{min}_{x_c,i}, \mathrm{x}^{max}_{x_c,i}, \mathrm{y}^{min}_{y_c,i}$ and $\mathrm{y}^{max}_{y_c,i}$.

Finally, we define $o(L_i(x_c,y_c))$ as

$$o(L_i(x_c,y_c)) = \frac{1}{A_{c,i}} \sum_{\mathrm{x}=\mathrm{x}^{min}_{x_c,i}}^{\mathrm{x}^{max}_{x_c,i}} \sum_{\mathrm{y}=\mathrm{y}^{min}_{y_c,i}}^{\mathrm{y}^{max}_{y_c,i}} B(\mathrm{x},\mathrm{y})$$

with

$$A_{c,i} = (\mathrm{x}^{max}_{x_c,i} - \mathrm{x}^{min}_{x_c,i} + 1)(\mathrm{y}^{max}_{y_c,i} - \mathrm{y}^{min}_{y_c,i} + 1).$$

Clearly, the more important the content which is occupied by a detail lens L_i when it is placed at cell c, the bigger the value $o(L_i(x_c,y_c))$, and therefore the smaller the quality value q_{τ,i,x_c,y_c} (assuming the distance $d(L_i(x_c,y_c),P_i)$ is kept fixed).

2 BIP Simplification

After the merge, the new n^* hard constraints replace the hard constraints of type **C1**, **C3**, and **C4** in the following way:

- The purpose of the hard constraints **C1**, which is showing each detail lens L_i just once at a time, is achieved since, if L_i was shown twice at one particular frame τ, this would imply that L_i is visible at frame τ at two different grid cells c and c'. This in turn would imply that L_i appears and disappears at c and c', making a sum of 4 and therefore violating the constraint.
- The purpose of the hard constraints **C3**, which is showing each detail lens L_i at just one position on the map, is achieved for a similar reason than why the goal of hard constraints **C1** is achieved: If there was a jump of a detail lens L_i, it would be visible at a grid cell c for one or more consecutive frames, and then at another grid cell c' for some later frames. This again would imply that L_i appears and disappears at c and c', making a sum of 4 and therefore violating the constraint.
- Finally, the purpose of the hard constraints **C4**, which is showing each detail lens L_i in just one contiguous block of frames, is achieved since we could already show that the hard constraints **C1** and **C3** are met by the new constraints, thereby placing the detail lens L_i at most once per frame at one particular grid cell c, which leads to a reduction of the set of variables that can have a value of 1 to those which correspond to the grid cell c. This leads to the exact definition of the hard constraints **C4**.

3 Detail Lens Placement

In the following we present a more detailed derivation of the hard constraints of type **C4**, which are introduced to avoid any flickering artifacts caused by permanent appearance and disappearance, thereby showing each detail lens in just one contiguous block of frames.

We start with an informal definition including an absolute value which can therefore not be directly introduced to the BIP:

$$v_{1,i,x_c,y_c} + \sum_{\tau=2}^{\tau_{max}} |v_{\tau,i,x_c,y_c} - v_{\tau-1,i,x_c,y_c}| + v_{\tau_{\max},i,x_c,y_c} = 2$$
$$i \in [1,n^*]; c \in C$$

We base the definition of the $n^* \cdot |C|$ hard constraints of type **C4** on the observation that if a detail lens L_i is visible at just one grid cell c (ensured by hard constraint **C3**) in just one contiguous block of frames, it appears once, stays visible for a certain number of frames, and finally disappears and stays invisible until the end of the visualization. When keeping the index i and the cell c fixed to continue this example and taking a look at the values of the neighboring variables along the time axis for $1 \leq \tau \leq \tau_{\max}$, this behavior corresponds to a certain number of variables v_{τ,i,x_c,y_c} being 0, followed by some variables being 1, followed by a sequence of variables which are 0 again. If now we applied the backward difference operator for $2 \leq \tau \leq \tau_{\max}$ and sum up the absolute values of all differences, we would get a value of 2.

There are, however, two special cases which are not considered in this observation, and these are the cases when a detail lens is visible directly from the beginning ($v_{1,i,x_c,y_c} = 1$) or visible until the end ($v_{\tau_{\max},i,x_c,y_c} = 1$). To incorporate these cases, we have to add the absolute differences between the variables of frame $\tau = 1$ and the non-existing frame $\tau = 0$, which is known to be 0, as well as frame $\tau = \tau_{\max}$ and the non-existing frame $\tau = \tau_{\max} + 1$, which

k	Mooney and Winstanley [2006] $q(\mathbf{p})$	Length [m]	Comp. [s]	Lu et al. [2010] $q(\mathbf{p})$	Length [m]	Comp. [s]	Kachkaev and Wood [2014] $q(\mathbf{p})$	Length [m]	Comp. [s]	**Our Approach** $q(\mathbf{p})$	Length [m]	Comp. [s]
8	10,00	540,98	8,58	1,50	67,94	106,96	1,50	67,94	0,01	10,00	540,98	0,30
16	23,00	1068,70	5,80	19,00	738,52	62368,66	1,50	67,94	0,01	23,00	1064,77	5,70
32	64,50	2171,23	14,88	N/A	N/A	N/A	1,50	67,94	0,01	71,00	2142,78	7,26
64	106,50	4347,50	14,60	N/A	N/A	N/A	1,50	67,94	0,01	141,00	4347,83	2,00
128	136,00	6790,82	13,68	N/A	N/A	N/A	1,50	67,94	0,01	190,50	8342,93	0,47

TABLE 1: Performance values of several path computation algorithms for the example shown in Figure 4. The column $q(\mathbf{p})$ refers to the quality of the computed path $\mathbf{p}$, Length [m] to the length in meters, and Comp. [s] to the computation time in seconds. The number k defines the maximum walking distance via $\delta_{\max} = k \cdot \delta_{\min}$ with $\delta_{\min} = 67.935$ m.

is known to be 0 as well. Those two missing absolute differences can therefore simply be considered by including the values of the variables v_{1,i,x_c,y_c} and $v_{\tau_{\max},i,x_c,y_c}$, which leads us to the definition of Equation 3.

The absolute value used in the sum in Equation 3 is however not permitted, but it is possible to rewrite the definition to get a formulation that can be introduced to the BIP. To this end we first have to introduce a set of new binary helper variables d_{τ,i,x_c,y_c}, which represent the absolute value of differences between neighboring variables v_{τ,i,x_c,y_c} and $v_{\tau-1,i,x_c,y_c}$ with respect to the time axis. Further, we have to introduce the following constraints to the BIP:

$$d_{\tau,i,x_c,y_c} \geq v_{\tau,i,x_c,y_c} - v_{\tau-1,i,x_c,y_c}$$
$$d_{\tau,i,x_c,y_c} \geq v_{\tau-1,i,x_c,y_c} - v_{\tau,i,x_c,y_c}$$
$$i \in [1, n^*]; \tau \in [2, \tau_{\max}]; c \in C$$

Clearly, due to the two constraints every binary helper variable d_{τ,i,x_c,y_c} has to meet, the value of d_{τ,i,x_c,y_c} will always be at least as big as the absolute value of the difference of the two corresponding variables. In fact, the value of d_{τ,i,x_c,y_c} will always *exactly* resemble the absolute value of the difference, since the objective function wants to maximize the number of variables which become 1, which is only possible when the variables d_{τ,i,x_c,y_c} are as small as possible. To complete the definition of the hard constraints of type **C4**, the binary helper variables are used to achieve the desired behavior.

4 Path Computation - Details

In Table 1 and Figures 1 and 4 we compare our BIP-based path computation approach to several competing methods for an example with very small distance between origin and destination. Note that all shown results are valid paths without any self-intersections (cf. zoom-in to the apparent intersection in the wrapped figure). We did not include the results of the approach of Kachkaev and Wood [2014] in the figures since it delivered the shortest path in all cases. Their method leverages Dijkstra's shortest path algorithm in an iterative manner with special edge weights to find a high-quality path. In detail, they gradually reduce the weights representing distance values with increasing iteration number according to

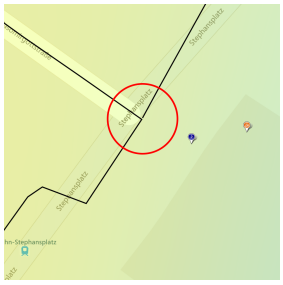

$$\omega(e_k) = l(e_k)(1 - \min(1, c \cdot q_k/\bar{q})) \quad (1)$$

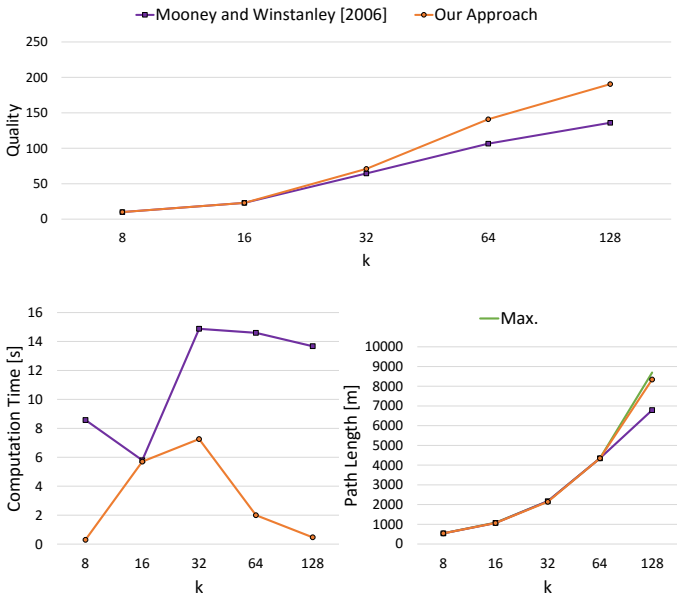

Fig. 1: Comparison of our path computation approach to the approach of Mooney and Winstanley [2006] which represents the only competing method that delivered good results in suitable time. For their method, we chose $N = 1000$, $G = 500$ and the generational change parameter $\alpha = 0.25$ which causes a termination if $\alpha \cdot G = 0.25 \cdot 500 = 125$ generations of solutions can not increase the path quality. The horizontal axis corresponds to the maximum walking distance $\delta_{\max} = k \cdot \delta_{\min}$. This distance is used as a hard constraint for all algorithms.

where $\omega(e_k)$ is the weight, $l(e_k)$ is the geographic distance and q_k is the quality of the edge e_k. The value c is the quality influence that is increased proportionally to the iteration number and $\bar{q}$ is the average quality value.

We stated in the paper that their method fails on our toy example. The reason for this failure is illustrated in Figure 2. Only a quality influence of 100% with $c = \bar{q}/\min_k\{q_k | q_k > 0\}$ can alter the edge weights such that the optimal solution corresponds to the shortest path. This, however, sets all edge weights equal to 0 and makes the path choice arbitrary. The fact that the algorithm of Kachkaev and Wood [2014] also fails in the example shown in Figure 4, is a result of the fact that user position and destination are close together. Moreover, since in our approach only edges that are adjacent to nearby POIs have a quality value > 0, many edges remain with $q = 0$ and are therefore untouched by Equation 1. This behavior is shown in Figure 3.

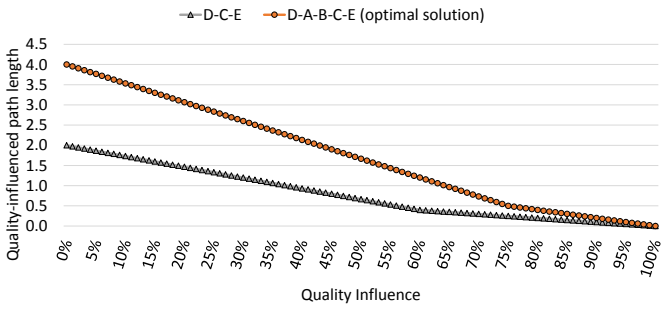

Fig. 2: The approach of Kachkaev and Wood [2014] which leverages Dijkstra's shortest path algorithm only finds a sub-optimal solution (shown in gray) in our toy example since it always corresponds to the shortest path, no matter how strong the quality values influence the distance values. Only with an influence value of 100% the length reaches the optimum, which however sets all edge weights equal to 0 and makes the path choice arbitrary.

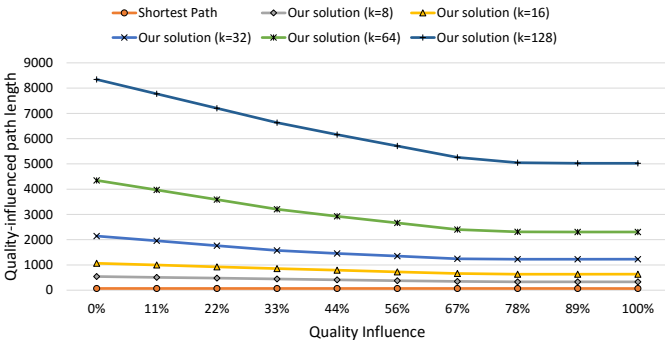

Fig. 3: The approach of Kachkaev and Wood [2014] only finds the shortest path for all k defining the maximum walking distance $\delta_{\max} = k \cdot \delta_{\min}$ in the example shown in Figure 4, no matter how strong the quality values influence the distance values. The reason for this behavior is the short distance between user position and destination and many edges in the graph whose weight is untouched by Equation 1 due to a quality value 0. As a result, the geographic shortest path always corresponds to the shortest path, also when the edge weights are reduced using the quality values.

The approach of Lu et al. [2010] utilizes dynamic programming and tries to find an optimal path between two nodes s and d by finding a node k such that the optimum from s to d can be combined using the two optimal paths from s to k and from k to d. The complexity level of their approach is $\mathcal{O}\left(|V|^3\,(\delta_{\max}/step)^2\right)$, with $|V|$ being the number of vertices, and $step$ being a parameter denoting the atomic path length (e.g. 10 m).

5 First User Study - Details

In the following we present more details about the results of the first user study which were not already shown in the paper. The aim of the first user study was the evaluation of the algorithm that is used in our framework for detail lens placement.

5.1 Off-diagonal matrices M^k

In this section we list all matrices M^k for each user k that participated in the first user study. As a reminder, the results of each participant k were translated into an off-diagonal 5×5 matrix M^k with entries M^k_{ij} corresponding to the number of times method j was preferred to method i. By summing up the columns, we identify the number of points which were distributed to the methods by the participants. The numbers between parentheses correspond to the algorithms which were tested in the study:

1) Complete optimized placement.
2) Incremental placement with 4 parts.
3) Incremental placement with 8 parts.
4) Naïve placement per frame without temporal coherence.
5) Complete optimized placement in screen space.

$$M^1 = \begin{array}{c} \\ (1) \\ (2) \\ (3) \\ (4) \\ (5) \\ \Sigma \end{array} \begin{array}{c} \begin{array}{ccccc} (1) & (2) & (3) & (4) & (5) \end{array} \\ \begin{pmatrix} - & 3 & 2 & 1 & 0 \\ 2 & - & 3 & 1 & 3 \\ 3 & 2 & - & 0 & 2 \\ 4 & 4 & 5 & - & 1 \\ 5 & 2 & 3 & 4 & - \end{pmatrix} \\ \begin{array}{ccccc} \mathbf{14} & \mathbf{11} & \mathbf{13} & \mathbf{6} & \mathbf{6} \end{array} \end{array}$$

$$M^2 = \begin{array}{c} \\ (1) \\ (2) \\ (3) \\ (4) \\ (5) \\ \Sigma \end{array} \begin{array}{c} \begin{array}{ccccc} (1) & (2) & (3) & (4) & (5) \end{array} \\ \begin{pmatrix} - & 1 & 3 & 0 & 2 \\ 4 & - & 2 & 1 & 4 \\ 2 & 3 & - & 0 & 5 \\ 5 & 4 & 5 & - & 5 \\ 3 & 1 & 0 & 0 & - \end{pmatrix} \\ \begin{array}{ccccc} \mathbf{14} & \mathbf{9} & \mathbf{10} & \mathbf{1} & \mathbf{16} \end{array} \end{array}$$

$$M^3 = \begin{array}{c} \\ (1) \\ (2) \\ (3) \\ (4) \\ (5) \\ \Sigma \end{array} \begin{array}{c} \begin{array}{ccccc} (1) & (2) & (3) & (4) & (5) \end{array} \\ \begin{pmatrix} - & 3 & 3 & 0 & 0 \\ 2 & - & 3 & 0 & 2 \\ 2 & 2 & - & 0 & 0 \\ 5 & 5 & 5 & - & 3 \\ 5 & 3 & 5 & 2 & - \end{pmatrix} \\ \begin{array}{ccccc} \mathbf{14} & \mathbf{13} & \mathbf{16} & \mathbf{2} & \mathbf{5} \end{array} \end{array}$$

$$M^4 = \begin{array}{c} \\ (1) \\ (2) \\ (3) \\ (4) \\ (5) \\ \Sigma \end{array} \begin{array}{c} \begin{array}{ccccc} (1) & (2) & (3) & (4) & (5) \end{array} \\ \begin{pmatrix} - & 0 & 1 & 0 & 0 \\ 5 & - & 1 & 0 & 0 \\ 4 & 4 & - & 0 & 0 \\ 5 & 5 & 5 & - & 5 \\ 5 & 5 & 5 & 0 & - \end{pmatrix} \\ \begin{array}{ccccc} \mathbf{19} & \mathbf{14} & \mathbf{12} & \mathbf{0} & \mathbf{5} \end{array} \end{array}$$

$$M^5 = \begin{array}{c} \\ (1) \\ (2) \\ (3) \\ (4) \\ (5) \\ \Sigma \end{array} \begin{array}{c} \begin{array}{ccccc} (1) & (2) & (3) & (4) & (5) \end{array} \\ \begin{pmatrix} - & 3 & 3 & 2 & 4 \\ 2 & - & 3 & 0 & 2 \\ 2 & 2 & - & 2 & 4 \\ 3 & 5 & 3 & - & 4 \\ 1 & 3 & 1 & 1 & - \end{pmatrix} \\ \begin{array}{ccccc} \mathbf{8} & \mathbf{13} & \mathbf{10} & \mathbf{5} & \mathbf{14} \end{array} \end{array}$$

$$M^6 = \begin{array}{c} \\ (1) \\ (2) \\ (3) \\ (4) \\ (5) \\ \Sigma \end{array} \begin{array}{c} \begin{array}{ccccc} (1) & (2) & (3) & (4) & (5) \end{array} \\ \begin{pmatrix} - & 5 & 2 & 1 & 5 \\ 0 & - & 0 & 0 & 5 \\ 3 & 5 & - & 1 & 5 \\ 4 & 5 & 4 & - & 5 \\ 0 & 0 & 0 & 0 & - \end{pmatrix} \\ \begin{array}{ccccc} \mathbf{7} & \mathbf{15} & \mathbf{6} & \mathbf{2} & \mathbf{20} \end{array} \end{array}$$

$$M^7 = \begin{array}{c} \\ (1) \\ (2) \\ (3) \\ (4) \\ (5) \\ \Sigma \end{array} \begin{array}{c} \begin{array}{ccccc} (1) & (2) & (3) & (4) & (5) \end{array} \\ \begin{pmatrix} - & 1 & 2 & 1 & 0 \\ 4 & - & 2 & 0 & 0 \\ 3 & 3 & - & 0 & 2 \\ 4 & 5 & 5 & - & 5 \\ 5 & 5 & 3 & 0 & - \end{pmatrix} \\ \begin{array}{ccccc} \mathbf{16} & \mathbf{14} & \mathbf{12} & \mathbf{1} & \mathbf{7} \end{array} \end{array}$$

$$M^8 = \begin{array}{c} \\ (1) \\ (2) \\ (3) \\ (4) \\ (5) \\ \Sigma \end{array} \begin{array}{c} \begin{array}{ccccc} (1) & (2) & (3) & (4) & (5) \end{array} \\ \begin{pmatrix} - & 2 & 2 & 0 & 0 \\ 3 & - & 2 & 0 & 0 \\ 3 & 3 & - & 0 & 0 \\ 5 & 5 & 5 & - & 5 \\ 5 & 5 & 5 & 0 & - \end{pmatrix} \\ \begin{array}{ccccc} \mathbf{16} & \mathbf{15} & \mathbf{14} & \mathbf{0} & \mathbf{5} \end{array} \end{array}$$

$$M^9 = \begin{array}{c} \\ (1) \\ (2) \\ (3) \\ (4) \\ (5) \\ \Sigma \end{array} \begin{array}{c} \begin{array}{ccccc} (1) & (2) & (3) & (4) & (5) \end{array} \\ \begin{pmatrix} - & 2 & 3 & 0 & 0 \\ 3 & - & 3 & 0 & 0 \\ 2 & 2 & - & 0 & 0 \\ 5 & 5 & 5 & - & 5 \\ 5 & 5 & 5 & 0 & - \end{pmatrix} \\ \begin{array}{ccccc} \mathbf{15} & \mathbf{14} & \mathbf{16} & \mathbf{0} & \mathbf{5} \end{array} \end{array}$$

$$M^{10} = \begin{array}{c} \\ (1) \\ (2) \\ (3) \\ (4) \\ (5) \\ \Sigma \end{array} \begin{array}{c} \begin{array}{ccccc} (1) & (2) & (3) & (4) & (5) \end{array} \\ \begin{pmatrix} - & 2 & 3 & 0 & 1 \\ 3 & - & 5 & 0 & 0 \\ 2 & 0 & - & 0 & 1 \\ 5 & 5 & 5 & - & 5 \\ 4 & 5 & 4 & 0 & - \end{pmatrix} \\ \begin{array}{ccccc} \mathbf{14} & \mathbf{12} & \mathbf{17} & \mathbf{0} & \mathbf{7} \end{array} \end{array}$$

$$M^{11} = \begin{array}{c} \\ (1) \\ (2) \\ (3) \\ (4) \\ (5) \\ \Sigma \end{array} \begin{array}{c} \begin{array}{ccccc} (1) & (2) & (3) & (4) & (5) \end{array} \\ \begin{pmatrix} - & 1 & 2 & 5 & 0 \\ 4 & - & 1 & 5 & 0 \\ 3 & 4 & - & 5 & 0 \\ 0 & 0 & 0 & - & 0 \\ 5 & 5 & 5 & 5 & - \end{pmatrix} \\ \begin{array}{ccccc} \mathbf{12} & \mathbf{10} & \mathbf{8} & \mathbf{20} & \mathbf{0} \end{array} \end{array}$$

$$M^{12} = \begin{array}{c} \\ (1) \\ (2) \\ (3) \\ (4) \\ (5) \\ \Sigma \end{array} \begin{array}{c} \begin{array}{ccccc} (1) & (2) & (3) & (4) & (5) \end{array} \\ \begin{pmatrix} - & 1 & 2 & 1 & 2 \\ 4 & - & 4 & 1 & 1 \\ 3 & 1 & - & 2 & 0 \\ 4 & 4 & 3 & - & 1 \\ 3 & 4 & 5 & 4 & - \end{pmatrix} \\ \begin{array}{ccccc} \mathbf{14} & \mathbf{10} & \mathbf{14} & \mathbf{8} & \mathbf{4} \end{array} \end{array}$$

$$M^{13} = \begin{array}{c} \\ (1) \\ (2) \\ (3) \\ (4) \\ (5) \\ \Sigma \end{array} \begin{array}{c} \begin{array}{ccccc} (1) & (2) & (3) & (4) & (5) \end{array} \\ \begin{pmatrix} - & 2 & 2 & 0 & 0 \\ 3 & - & 1 & 0 & 0 \\ 3 & 4 & - & 0 & 0 \\ 5 & 5 & 5 & - & 5 \\ 5 & 5 & 5 & 0 & - \end{pmatrix} \\ \begin{array}{ccccc} \mathbf{16} & \mathbf{16} & \mathbf{13} & \mathbf{0} & \mathbf{5} \end{array} \end{array}$$

$$M^{14} = \begin{array}{c} \\ (1) \\ (2) \\ (3) \\ (4) \\ (5) \\ \Sigma \end{array} \begin{array}{c} \begin{array}{ccccc} (1) & (2) & (3) & (4) & (5) \end{array} \\ \begin{pmatrix} - & 0 & 2 & 0 & 1 \\ 5 & - & 2 & 0 & 0 \\ 3 & 3 & - & 0 & 0 \\ 5 & 5 & 5 & - & 4 \\ 4 & 5 & 5 & 1 & - \end{pmatrix} \\ \begin{array}{ccccc} \mathbf{17} & \mathbf{13} & \mathbf{14} & \mathbf{1} & \mathbf{5} \end{array} \end{array}$$

$$M^{15} = \begin{array}{c} \\ (1) \\ (2) \\ (3) \\ (4) \\ (5) \\ \Sigma \end{array} \begin{array}{c} \begin{array}{ccccc} (1) & (2) & (3) & (4) & (5) \end{array} \\ \begin{pmatrix} - & 2 & 4 & 0 & 1 \\ 3 & - & 2 & 0 & 0 \\ 1 & 3 & - & 0 & 0 \\ 5 & 5 & 5 & - & 1 \\ 4 & 5 & 5 & 4 & - \end{pmatrix} \\ \begin{array}{ccccc} \mathbf{13} & \mathbf{15} & \mathbf{16} & \mathbf{4} & \mathbf{2} \end{array} \end{array}$$

$$M^{16} = \begin{array}{c} \\ (1) \\ (2) \\ (3) \\ (4) \\ (5) \\ \Sigma \end{array} \begin{array}{c} \begin{array}{ccccc} (1) & (2) & (3) & (4) & (5) \end{array} \\ \begin{pmatrix} - & 4 & 4 & 0 & 0 \\ 1 & - & 4 & 0 & 1 \\ 1 & 1 & - & 0 & 0 \\ 5 & 5 & 5 & - & 2 \\ 5 & 4 & 5 & 3 & - \end{pmatrix} \\ \begin{array}{ccccc} \mathbf{12} & \mathbf{14} & \mathbf{18} & \mathbf{3} & \mathbf{3} \end{array} \end{array}$$

$$M^{17}=\begin{array}{c}\\(1)\\(2)\\(3)\\(4)\\(5)\\\Sigma\end{array}\begin{array}{c}\begin{array}{ccccc}(1)&(2)&(3)&(4)&(5)\end{array}\\\begin{pmatrix}-&3&2&4&1\\2&-&1&3&2\\3&4&-&3&1\\1&2&2&-&1\\4&3&4&4&-\end{pmatrix}\\\begin{array}{ccccc}\mathbf{10}&\mathbf{12}&\mathbf{9}&\mathbf{14}&\mathbf{5}\end{array}\end{array}\quad M^{18}=\begin{array}{c}\\(1)\\(2)\\(3)\\(4)\\(5)\\\Sigma\end{array}\begin{array}{c}\begin{array}{ccccc}(1)&(2)&(3)&(4)&(5)\end{array}\\\begin{pmatrix}-&1&3&1&2\\4&-&2&1&3\\2&3&-&0&1\\4&4&5&-&3\\3&2&4&2&-\end{pmatrix}\\\begin{array}{ccccc}\mathbf{13}&\mathbf{10}&\mathbf{14}&\mathbf{4}&\mathbf{9}\end{array}\end{array}$$

$$M^{19}=\begin{array}{c}\\(1)\\(2)\\(3)\\(4)\\(5)\\\Sigma\end{array}\begin{array}{c}\begin{array}{ccccc}(1)&(2)&(3)&(4)&(5)\end{array}\\\begin{pmatrix}-&3&3&0&2\\2&-&2&0&1\\2&3&-&0&2\\5&5&5&-&5\\3&4&3&0&-\end{pmatrix}\\\begin{array}{ccccc}\mathbf{12}&\mathbf{15}&\mathbf{13}&\mathbf{0}&\mathbf{10}\end{array}\end{array}\quad M^{20}=\begin{array}{c}\\(1)\\(2)\\(3)\\(4)\\(5)\\\Sigma\end{array}\begin{array}{c}\begin{array}{ccccc}(1)&(2)&(3)&(4)&(5)\end{array}\\\begin{pmatrix}-&2&1&0&1\\3&-&3&0&0\\4&2&-&0&1\\5&5&5&-&4\\4&5&4&1&-\end{pmatrix}\\\begin{array}{ccccc}\mathbf{16}&\mathbf{14}&\mathbf{13}&\mathbf{1}&\mathbf{6}\end{array}\end{array}$$

$$M^{21}=\begin{array}{c}\\(1)\\(2)\\(3)\\(4)\\(5)\\\Sigma\end{array}\begin{array}{c}\begin{array}{ccccc}(1)&(2)&(3)&(4)&(5)\end{array}\\\begin{pmatrix}-&2&4&1&0\\3&-&1&0&1\\1&4&-&0&0\\4&5&5&-&1\\5&4&5&4&-\end{pmatrix}\\\begin{array}{ccccc}\mathbf{13}&\mathbf{15}&\mathbf{15}&\mathbf{5}&\mathbf{2}\end{array}\end{array}\quad M^{22}=\begin{array}{c}\\(1)\\(2)\\(3)\\(4)\\(5)\\\Sigma\end{array}\begin{array}{c}\begin{array}{ccccc}(1)&(2)&(3)&(4)&(5)\end{array}\\\begin{pmatrix}-&3&1&2&0\\2&-&2&2&0\\4&3&-&2&1\\3&3&3&-&3\\5&5&4&2&-\end{pmatrix}\\\begin{array}{ccccc}\mathbf{14}&\mathbf{14}&\mathbf{10}&\mathbf{8}&\mathbf{4}\end{array}\end{array}$$

$$M^{23}=\begin{array}{c}\\(1)\\(2)\\(3)\\(4)\\(5)\\\Sigma\end{array}\begin{array}{c}\begin{array}{ccccc}(1)&(2)&(3)&(4)&(5)\end{array}\\\begin{pmatrix}-&3&2&1&5\\2&-&2&1&3\\3&3&-&1&1\\4&4&4&-&5\\0&2&4&0&-\end{pmatrix}\\\begin{array}{ccccc}\mathbf{9}&\mathbf{12}&\mathbf{12}&\mathbf{3}&\mathbf{14}\end{array}\end{array}\quad M^{24}=\begin{array}{c}\\(1)\\(2)\\(3)\\(4)\\(5)\\\Sigma\end{array}\begin{array}{c}\begin{array}{ccccc}(1)&(2)&(3)&(4)&(5)\end{array}\\\begin{pmatrix}-&2&0&0&2\\3&-&2&0&1\\5&3&-&0&5\\5&5&5&-&5\\3&4&0&0&-\end{pmatrix}\\\begin{array}{ccccc}\mathbf{16}&\mathbf{14}&\mathbf{7}&\mathbf{0}&\mathbf{13}\end{array}\end{array}$$

$$M^{25}=\begin{array}{c}\\(1)\\(2)\\(3)\\(4)\\(5)\\\Sigma\end{array}\begin{array}{c}\begin{array}{ccccc}(1)&(2)&(3)&(4)&(5)\end{array}\\\begin{pmatrix}-&5&3&0&1\\0&-&2&0&2\\2&3&-&0&0\\5&5&5&-&4\\4&3&5&1&-\end{pmatrix}\\\begin{array}{ccccc}\mathbf{11}&\mathbf{16}&\mathbf{15}&\mathbf{1}&\mathbf{7}\end{array}\end{array}\quad M^{26}=\begin{array}{c}\\(1)\\(2)\\(3)\\(4)\\(5)\\\Sigma\end{array}\begin{array}{c}\begin{array}{ccccc}(1)&(2)&(3)&(4)&(5)\end{array}\\\begin{pmatrix}-&3&1&1&1\\2&-&3&0&1\\4&2&-&2&1\\4&5&3&-&3\\4&4&4&2&-\end{pmatrix}\\\begin{array}{ccccc}\mathbf{14}&\mathbf{14}&\mathbf{11}&\mathbf{5}&\mathbf{6}\end{array}\end{array}$$

$$M^{27}=\begin{array}{c}\\(1)\\(2)\\(3)\\(4)\\(5)\\\Sigma\end{array}\begin{array}{c}\begin{array}{ccccc}(1)&(2)&(3)&(4)&(5)\end{array}\\\begin{pmatrix}-&2&3&0&1\\3&-&2&0&0\\2&3&-&0&2\\5&5&5&-&4\\4&5&3&1&-\end{pmatrix}\\\begin{array}{ccccc}\mathbf{14}&\mathbf{15}&\mathbf{13}&\mathbf{1}&\mathbf{7}\end{array}\end{array}\quad M^{28}=\begin{array}{c}\\(1)\\(2)\\(3)\\(4)\\(5)\\\Sigma\end{array}\begin{array}{c}\begin{array}{ccccc}(1)&(2)&(3)&(4)&(5)\end{array}\\\begin{pmatrix}-&1&1&4&2\\4&-&2&2&2\\4&3&-&4&1\\1&3&1&-&2\\3&3&4&3&-\end{pmatrix}\\\begin{array}{ccccc}\mathbf{12}&\mathbf{10}&\mathbf{8}&\mathbf{13}&\mathbf{7}\end{array}\end{array}$$

$$M^{29}=\begin{array}{c}\\(1)\\(2)\\(3)\\(4)\\(5)\\\Sigma\end{array}\begin{array}{c}\begin{array}{ccccc}(1)&(2)&(3)&(4)&(5)\end{array}\\\begin{pmatrix}-&3&2&1&2\\2&-&2&2&2\\3&3&-&1&4\\4&3&4&-&3\\3&3&1&2&-\end{pmatrix}\\\begin{array}{ccccc}\mathbf{12}&\mathbf{12}&\mathbf{9}&\mathbf{6}&\mathbf{11}\end{array}\end{array}\quad M^{30}=\begin{array}{c}\\(1)\\(2)\\(3)\\(4)\\(5)\\\Sigma\end{array}\begin{array}{c}\begin{array}{ccccc}(1)&(2)&(3)&(4)&(5)\end{array}\\\begin{pmatrix}-&2&1&0&0\\3&-&1&1&0\\4&4&-&0&0\\5&4&5&-&0\\5&5&5&5&-\end{pmatrix}\\\begin{array}{ccccc}\mathbf{17}&\mathbf{15}&\mathbf{12}&\mathbf{6}&\mathbf{0}\end{array}\end{array}$$

$$M^{31}=\begin{array}{c}\\1)\\(2)\\(3)\\(4)\\(5)\\\Sigma\end{array}\begin{array}{c}\begin{array}{ccccc}(1)&(2)&(3)&(4)&(5)\end{array}\\\begin{pmatrix}-&3&2&0&0\\2&-&1&0&0\\3&4&-&0&0\\5&5&5&-&5\\5&5&5&0&-\end{pmatrix}\\\begin{array}{ccccc}\mathbf{15}&\mathbf{17}&\mathbf{13}&\mathbf{0}&\mathbf{5}\end{array}\end{array}\quad M^{32}=\begin{array}{c}\\(1)\\(2)\\(3)\\(4)\\(5)\\\Sigma\end{array}\begin{array}{c}\begin{array}{ccccc}(1)&(2)&(3)&(4)&(5)\end{array}\\\begin{pmatrix}-&2&3&3&0\\3&-&2&4&2\\2&3&-&2&2\\2&1&3&-&1\\5&3&3&4&-\end{pmatrix}\\\begin{array}{ccccc}\mathbf{12}&\mathbf{9}&\mathbf{11}&\mathbf{13}&\mathbf{5}\end{array}\end{array}$$

$$\sum_{k=1}^{32}M^k=\begin{array}{c}\\(1)\\(2)\\(3)\\(4)\\(5)\\\Sigma\\\mathbf{Avg}\end{array}\begin{array}{c}\begin{array}{ccccc}(1)&(2)&(3)&(4)&(5)\end{array}\\\begin{pmatrix}-&72&72&29&36\\88&-&68&24&38\\88&92&-&25&41\\131&136&135&-&105\\124&122&119&55&-\end{pmatrix}\\\begin{array}{ccccc}\mathbf{431}&\mathbf{422}&\mathbf{394}&\mathbf{133}&\mathbf{220}\\\mathbf{13.47}&\mathbf{13.19}&\mathbf{12.31}&\mathbf{4.16}&\mathbf{6.88}\end{array}\end{array}\tag{2}$$

By summing up all matrices M^k shown above we arrive at the matrix shown in Equation 2 that represents the total distribution of points to the algorithms. By performing an ANOVA and using the outcome to perform Tukey's honest significance test we can easily show that our proposed method in all its variants ((1), (2), and (3)) is preferred significantly to a screen space solution (5) and a naive solution (4) in which the detail lenses are positioned without temporal coherence per frame (cf. Figure 10 in the paper).

6 Second User Study - Evaluation

In Figure 5 we show the remaining results of the questionnaire that was handed to the participants of the second user study. Analogously to the paper, for easier notation we refer to the re-implemented Yelp functionality in our framework by simply using the term Yelp. Note that we did not tell the participants of the user study which method was the proposed method and which one was the re-implementation of the Yelp functionalities but we only used the terms "Method 1" and "Methods 2" in order to avoid any bias in the results.

As can be seen in Figure 5a, 58% of the participants agreed or strongly agreed that it is easy to find the correspondences between map pins and detail lenses. Although 83% had at least a neutral opinion, we still see room for improvement to make a matching of map pins and the corresponding information easier. Even though we consciously omitted leader lines between map pins and detail lenses in our design choices to avoid visual clutter, we plan to test how user performance and preference vary when the proposed solutions are compared to solutions which include leader lines. Another direction we want to explore and where we see interesting possibilities of future work are the usage of different colors or other visual hints that make a matching task easier.

Figure 5b shows that 58% of the participants think that an offset of the viewport w.r.t. the user position pin improves the visualization quality. This is achieved in our framework by the computation of a path for the map cutouts that represents the viewports in the final visualization.

Figure 5c shows the acceptance rate of the dynamic appearance and disappearance of the detail lenses in our visualizations. Although people are known to attend to movement at the edge of the field of view and may be distracted by the dynamic nature of the lenses, 75% agree or strongly agree that this design choice improves the visualization quality.

Since we wanted to know if our system could completely replace Yelp for exploration tasks, we asked the participants if they would use our proposed method only in addition to Yelp. 50% strongly disagreed or disagreed and 83% had at least a neutral opinion (cf. Figure 5d).

Another aspect of our system that we wanted to evaluate during the second user study was the size of the detail lenses. As can be seen in Figure 5e, our empirically estimated lens size seems to fit the preference of the users since 100% of the participants had at most a neutral opinion about the statement, that the lenses should be bigger, while at the same time 92% had at most a neutral opinion about smaller lenses.

Finally, we asked the participants if they think that it is possible to gather more information about the POIs (e.g. rankings) in the same time than with Yelp. As shown in Figure 5f, 83% of the participants agreed or strongly agreed.

7 Results

Figure 6 shows additional examples of our approach for several cities using different mobile output devices.

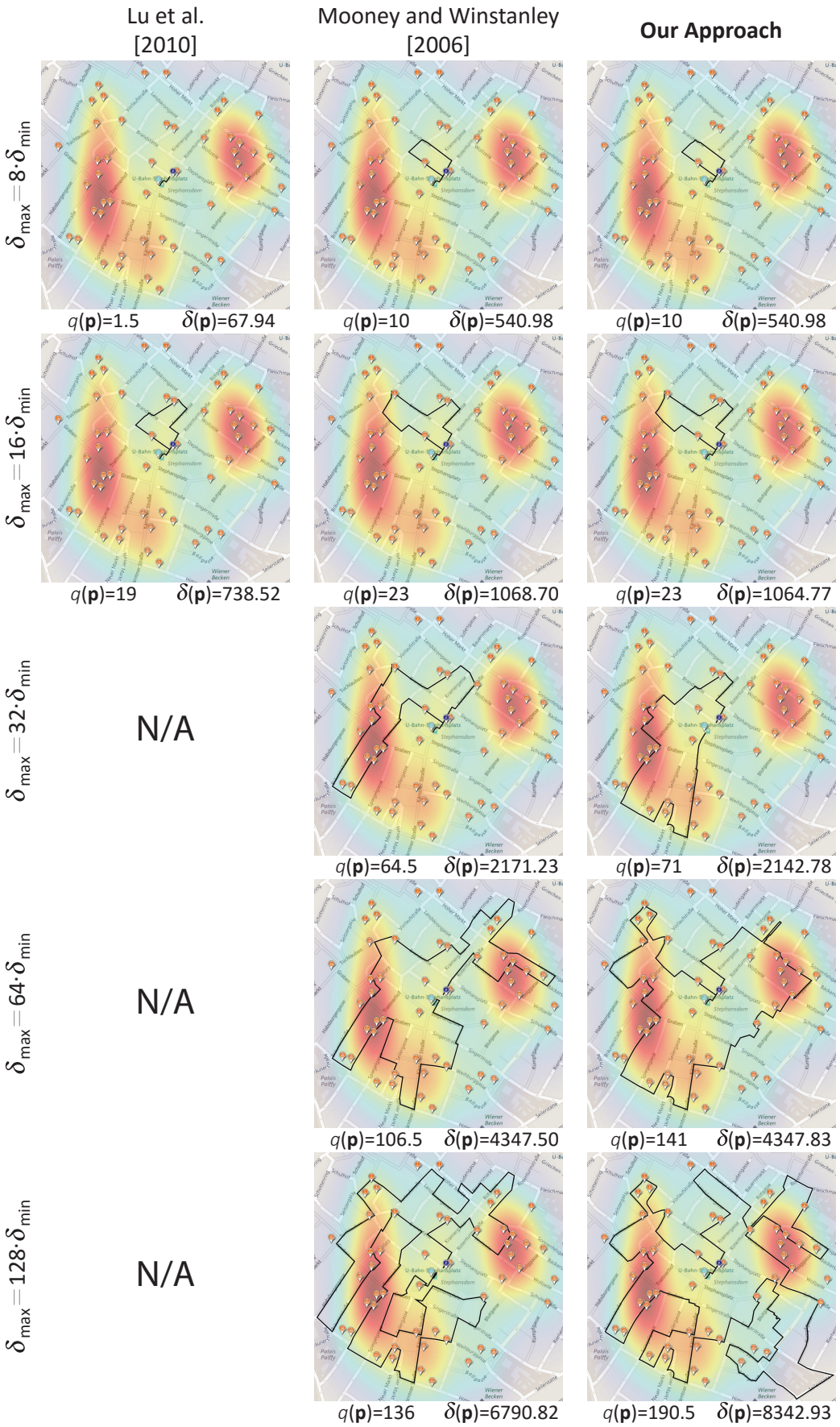

Fig. 4: Comparison of our BIP-based path computation approach to several competing methods for an example with very small distance between origin and destination (≈ 60 m). We skipped the computation of the results of the method of Lu et al. [2010] for $\delta_{\max} = k \cdot \delta_{\min}$ for $k > 16$ due to the long runtime (> 17.5 h). The only method beside ours that produced good results in a suitable time is the evolutionary algorithm by Mooney and Winstanley [2006]. However, our approach not only produced results with higher quality value, but it could also beat the runtime of their approach in all cases (cf. Table 1)

Fig. 5: The participants of the second study were asked to assign levels of agreement (Strongly Disagree to Strongly Agree) to several statements. Above the remaining statements that were not presented in the paper and the corresponding answers are shown.

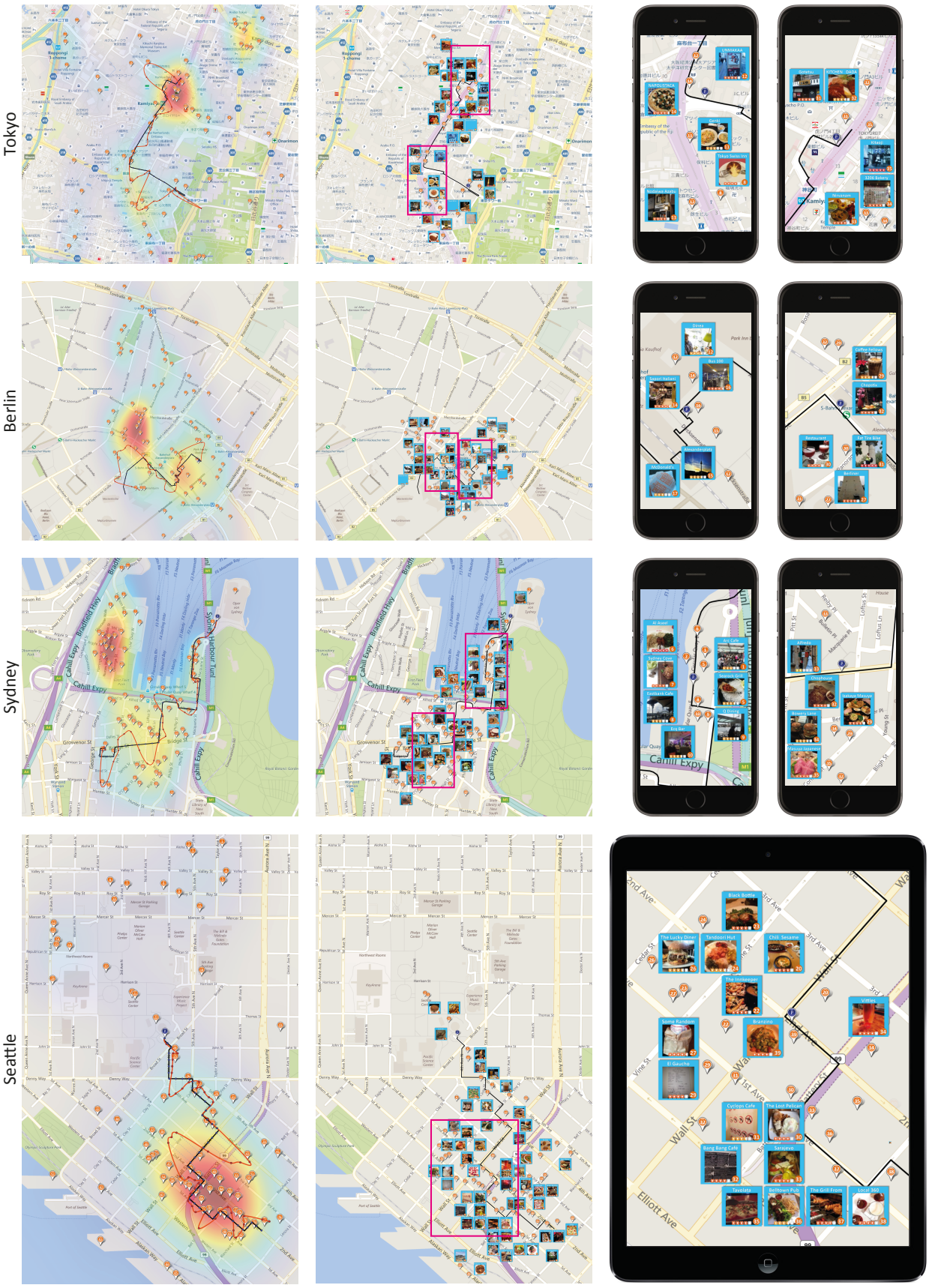

Fig. 6: Further results of our framework. (left) Overview of the example areas with the queried set of POIs P and the computed paths $\mathbf{p}(t)$ (black) and $\mathbf{m}(t)$ (dark orange). (middle) The computed positions of the detail lenses. (right) Example views of the final visualization for different mobile devices (iPhone 6 Plus and iPad Air 2).